Confined subdiffusion in three dimensions*

Qin Shan-Lin(覃善林) and He Yong(何 勇)†

Hunan Key Laboratory for Super-microstructure and Ultrafast Process, Institute of Super Microstructure and Ultrafast Process in Advanced Materials, School of Physics and Electronics, Central South University, Changsha 410012, *China*

(Received 19 March 2014; revised manuscript received 20 May 2014; published online 24 September 2014)

Three-dimensional (3D) Fick's diffusion equation and fractional diffusion equation are solved for different reflecting boundaries. We use the continuous time random walk model (CTRW) to investigate the time-averaged mean square displacement (MSD) of a 3D single particle trajectory. Theoretical results show that the ensemble average of the time-averaged MSD can be expressed analytically by a Mittag–Leffler function. Our new expression is in agreement with previous formulas in two limiting cases: $\langle\overline{\delta^2}\rangle \sim \Delta$ in short lag time and $\langle\overline{\delta^2}\rangle \sim \Delta^{1-\alpha}$ in long lag time. We also simulate the experimental data of mRNA diffusion in living E. coli using a 3D CTRW model under confined and crowded conditions. The simulation results are well consistent with experimental results. The calculations of power spectral density (PSD) further indicate the subdiffsive behavior of an individual trajectory.

Keywords: confined subdiffusion, three dimensions, time-averaged mean squared displacement

PACS: 02.50.−r, 05.10.Gg, 05.20.Dd **DOI:** 10.1088/1674-1056/23/11/110206

1. Introduction

Inside cells, the motion of the real biomolecules occurs in three dimensions. The three-dimensional (3D) trajectory tracking brings valuable information that is lost by two-dimensional (2D) tracking. Therefore, for an accurate determination of the diffusion, a 3D trajectory and analysis is required. Currently, the techniques of 3D single particle tracking (SPT)[1–10] enable us to observe the motion of a single particle with the position resolution of 3 nm and the time resolution of 100 ms.[4] But so far, the interpretation of experimental data was mostly restricted to one dimension. It is clear that there is a need for theory and simulation of microscopic models that can make quantitative predictions of the diffusion behaviour in three dimensions.

The diffusion environment of the single biomolecules in a living cell is confined and crowded. Roughly estimated, the sizes of the single biomolecules and the cell are from a few to several hundred nanometers and from one to one hundred micrometers, respectively. During diffusion, when a jumping biomolecule meets the cellular inner membrane, it will be reflected. So the diffusion is a confined motion. The cellular interior is also highly crowded. For example, a typical E. coli cell's geometrical size is about 1 μm × 1 μm × 2 μm, the volume $V \approx 1\ \mu m^3$. Inside an E. coli cell, there are about 2×10^6 proteins, 2×10^4 ribosomes, and 2×10^{10} water molecules. The mean spacing between protein molecules within an E. coli cell is less than 10 nanometers.[11]

The motion of single biomolecules inside a cell often exhibits subdiffusion with a slow diffusion coefficient in the confined and crowded environment. Up to now, for the interpretation of experimental results, three theoretical models are commonly employed.[12–16] The first approach is Gaussian models like fractional Brownian motion[17–20] and Langevin equations,[21–24] the second category is the continuous-time random walk,[25–30] and the last method is obstructed diffusion.[31–34] However, a thorough understanding of the microscopic mechanism of the single biomolecule's diffusion is still a challenge.[12–16,35,36]

We have applied the model of continuous time random walk (CTRW) to simulate[37,38] the experimental results[39] on the diffusion of mRNA molecules inside live E. coli. Recently, the large numbers of theoretical works have made remarkable headway in investigations on subdiffusion, especially on aging and weak ergodicity breaking.[14,15,40–47] Here we extend the previous 1D model[37,41] to 3D. We pay special attention to that case with different boundary conditions in three spatial directions.

The time-average mean squared displacement (MSD) $\overline{\delta_l^2}$ of the l-th trajectory is defined through a three-dimension trajectory $\boldsymbol{r}(t)$, which is recorded in the time interval $(0,T)$, according to

$$\overline{\delta_l^2}(\Delta,T) = \frac{1}{T-\Delta}\int_0^{T-\Delta}[\boldsymbol{r}(t+\Delta)-\boldsymbol{r}(t)]^2\,\mathrm{d}t, \qquad (1)$$

where $l = 1,2,\ldots,N$ labels the number of every different trajectory, T is the finite measurement time, and Δ denotes the lag time. The $\overline{\delta_l^2}$ can be obtained from a trajectory. From all N trajectories, we can obtain the ensemble average of the

*Project supported by the National Natural Science Foundation of China (Grant No. 21153002) and the Fundamental Research Funds for the Central Universities of China (Grant No. 2013zzts151).

†Corresponding author. E-mail: liuxizhong123@163.com

© 2014 Chinese Physical Society and IOP Publishing Ltd

time-averaged MSD

$$\langle\overline{\delta^2}(\Delta,T)\rangle = \lim_{N\to\infty}\frac{1}{N}\sum_{l=1}^{N}\overline{\delta_l^2}(\Delta,T) = \frac{1}{T-\Delta}\int_0^{T-\Delta}\langle[\boldsymbol{r}(t+\Delta)-\boldsymbol{r}(t)]^2\rangle\,\mathrm{d}t, \quad (2)$$

above, the angular brackets $\langle\cdot\rangle$ denotes the ensemble average. The ensemble average of a random walk can also be calculated in another way,

$$\left\langle[\boldsymbol{r}(t+\Delta)-\boldsymbol{r}(t)]^2\right\rangle = \int_V[\boldsymbol{r}(t+\Delta)-\boldsymbol{r}(t)]^2P(\boldsymbol{r};t)\,\mathrm{d}\boldsymbol{r}, \quad (3)$$

where the probability density function (PDF) $P(\boldsymbol{r};t)$ is the relative probability of finding the walker at the position $\boldsymbol{r}$ at time t. The $P(\boldsymbol{r};t)$ obeys the fractional diffusion equation[26,48] in three dimensions,

$$\frac{\partial}{\partial t}P(\boldsymbol{r};t) =_0 D_t^{1-\alpha}K_\alpha\bigtriangledown^2P(\boldsymbol{r};t), \quad (4)$$

where K_α is the diffusion constant, and the Riemann–Liouville operator is defined by[49]

$${}_0D_t^{1-\alpha}f(t) = \frac{1}{\Gamma(\alpha)}\frac{\partial}{\partial t}\int_0^t\frac{f(t')}{(t-t')^{1-\alpha}}\,\mathrm{d}t'. \quad (5)$$

We suppose that the cell has a cuboid shape with three side lengths L_x, L_y, and L_z in the rectangular coordinate system. The boundary condition and initial condition are imposed as

$$\begin{cases} P(\boldsymbol{r};t)|_{t=t_\mathrm{s}} = \delta(x-x_\mathrm{s})\delta(y-y_\mathrm{s})\delta(z-z_\mathrm{s}), \\ \dfrac{\partial}{\partial x}P(\boldsymbol{r};t)|_{x=0,x=L_x} = 0, \\ \dfrac{\partial}{\partial y}P(\boldsymbol{r};t)|_{y=0,y=L_y} = 0, \\ \dfrac{\partial}{\partial z}P(\boldsymbol{r};t)|_{z=0,z=L_z} = 0. \end{cases} \quad (6)$$

In this paper, we solve the three-dimensional (3D) Fick's diffusion equation and fractional diffusion equation with different reflecting boundaries. We use the continuous time random walk model (CTRW) to explore the time-averaged MSD of a 3D single particle trajectory. Theoretical results show the ensemble average of the time-averaged MSD can be expressed analytically by a Mittag-Leffler function. Our new expression is in agreement with previous formulas in two limiting cases which are $\langle\overline{\delta^2}\rangle\sim\Delta$ in the short lag time and $\langle\overline{\delta^2}\rangle\sim\Delta^{1-\alpha}$ in the long lag time. We also simulate the experimental data of mRNA diffusion in living E. coli using the 3D CTRW model under confined and crowded conditions. The simulated results are well consistent with experimental results. The calculations of power spectral density (PSD) indicate further the subdiffsive behavior of an individual trajectory.

2. Theoretical analysis

2.1. The exact solution of the 3D Fick's diffusion equation

We start from solving the 3D Fick's diffusion equation to calculate the ensemble-averaged MSD in three dimensions, which will be used to obtain the ensemble average of the time-averaged MSD later. The probability of finding the walker at position $\boldsymbol{r}$ at time t, if the walker was at position $\boldsymbol{r}_\mathrm{s}$ at time t_s, obeys Fick's diffusion equation

$$\frac{\partial}{\partial t}P(x,y,z,x_\mathrm{s},y_\mathrm{s},z_\mathrm{s};t,t_\mathrm{s}) = D\boldsymbol{\nabla}^2P(x,y,z,x_\mathrm{s},y_\mathrm{s},z_\mathrm{s};t,t_\mathrm{s}), \quad (7)$$

where D is the diffusion constant. According to the Einstein relation, D can be expressed by $D=\langle\delta r^2\rangle/2\langle t_\mathrm{w}\rangle$, where $\langle\delta r^2\rangle$ is the variance of the jump lengths and $\langle t_\mathrm{w}\rangle$ is the average waiting time for the normal diffusion. This function reasonably holds when $r^2\gg\langle\delta r^2\rangle$ and $t\gg\langle t_\mathrm{w}\rangle$.

When taking $t_\mathrm{s}=0$ and $0<x<L_x$, $0<y<L_y$, $0<z<L_z$, the initial condition and boundary condition are imposed as Eq. (6). Therefore, the solution of Eq. (7) is derived as

$$\begin{aligned} &P(x,y,z,x_\mathrm{s},y_\mathrm{s},z_\mathrm{s};t) \\ &= \sum_{n=0}^{\infty}\sum_{m=0}^{\infty}\sum_{k=0}^{\infty}\frac{2^{(\epsilon_{m0}+\epsilon_{n0}+\epsilon_{k0})}}{L_xL_yL_z}\cos\Big(\frac{n\pi x}{L_x}\Big)\cos\Big(\frac{m\pi y}{L_y}\Big)\cos\Big(\frac{k\pi z}{L_z}\Big) \\ &\quad\times\cos\Big(\frac{n\pi x_\mathrm{s}}{L_x}\Big)\cos\Big(\frac{m\pi y_\mathrm{s}}{L_y}\Big)\cos\Big(\frac{k\pi z_\mathrm{s}}{L_z}\Big) \\ &\quad\times\exp\Big\{-\Big[\Big(\frac{n\pi}{L_x}\Big)^2+\Big(\frac{m\pi}{L_y}\Big)^2+\Big(\frac{k\pi}{L_z}\Big)^2\Big]Dt\Big\}, \end{aligned} \quad (8)$$

where ϵ_{i0} is defined as

$$\epsilon_{i0} = \begin{cases} 1, & i\neq 0; \\ 0, & i=0, \end{cases} \quad i=m,\ n,\ \text{or}\ k. \quad (9)$$

2.2. The ensemble-averaged MSD for normal diffusion

For $r^2=x^2+y^2+z^2$, the ensemble-averaged MSD of normal diffusion, $\langle r^2(t)\rangle$, can be derived from Eq. (8) as

$$\begin{aligned} \langle r^2(t)\rangle &= \frac{1}{L_xL_yL_z}\int_0^{L_x}\int_0^{L_y}\int_0^{L_z}\mathrm{d}x_\mathrm{s}\,\mathrm{d}y_\mathrm{s}\,\mathrm{d}z_\mathrm{s}\int_0^{L_x}\int_0^{L_y}\int_0^{L_z}\mathrm{d}x\mathrm{d}y\mathrm{d}z \\ &\quad\times P(x,y,z,x_\mathrm{s},y_\mathrm{s},z_\mathrm{s};t)\left[(x-x_\mathrm{s})^2+(y-y_\mathrm{s})^2+(z-z_\mathrm{s})^2\right] \\ &= \frac{L_x^2+L_y^2+L_z^2}{6}+\sum_{n=0}^{\infty}\frac{16L_x^2}{(2n+1)^4\pi^4}\exp\Big[-\frac{(2n+1)^2\pi^2Dt}{L_x^2}\Big] \\ &\quad+\sum_{m=0}^{\infty}\frac{16L_y^2}{(2m+1)^4\pi^4}\exp\Big[-\frac{(2m+1)^2\pi^2Dt}{L_y^2}\Big] \\ &\quad+\sum_{k=0}^{\infty}\frac{16L_z^2}{(2k+1)^4\pi^4}\exp\Big[-\frac{(2k+1)^2\pi^2Dt}{L_z^2}\Big], \end{aligned} \quad (10)$$

when t is large, the ensemble-averaged MSD for normal diffusion reaches a constant $(L_x^2+L_y^2+L_z^2)/6$. The ensemble-averaged MSD of a confined random walker after $j=t/\langle t_\mathrm{w}\rangle$ jumps has the form

$$\langle r^2(j)\rangle = \sum_{i=0}^{\infty}\gamma_iq_i^j, \quad (11)$$

with $q_0 = 1$ and $q_i < 1$. The coefficients q_i and γ_i can be derived by comparison with Eq. (10).

2.3. The exact solution of 3D fractional diffusion equation

We can solve the 3D fractional diffusion equation by using the separation of variables.[41,50] Let

$$P(\boldsymbol{r};t) = X(x)Y(y)Z(z)T(t), \tag{12}$$

and substitute it back into Eq. (4), we obtain

$$\begin{cases} \dfrac{\partial^2 f(q)}{\partial q^2} = \lambda_q f(q), \\ \dfrac{\partial}{\partial q} f(q)|_{q=0,q=L_q} = 0, \end{cases} \tag{13}$$

$$\begin{cases} \dfrac{\partial}{\partial t} T(t) = -\lambda\ {}_0D_t^{1-\alpha} T(t), \\ T(t)|_{t=t_s} = 1, \end{cases} \tag{14}$$

where the coordinate $q = x$, y, or z, the function $f(q) = X(x)$, $Y(y)$, or $Z(z)$, and constant $\lambda = \lambda_x + \lambda_y + \lambda_z$. The initial condition is $P(\boldsymbol{r};t_s) = \delta(x-x_s)\delta(y-y_s)\delta(z-z_s)$. The solution of Eq. (4) should be labeled according to the choice of constants n, m, and k, that is,

$$P_{nmk}(\boldsymbol{r};t) = X_n(x)Y_m(y)Z_k(x)T_{nmk}(t). \tag{15}$$

The general solution is a linear combination of solutions P_{nmk},

$$\begin{aligned} P(\boldsymbol{r};t) &= \sum_{nmk=0}^{\infty} C_{nmk} P_{nmk}(x,y,z;t) \\ &= \sum_{n=0}^{\infty}\sum_{m=0}^{\infty}\sum_{k=0}^{\infty} \frac{2^{(\epsilon_{m0}+\epsilon_{n0}+\epsilon_{k0})}}{L_xL_yL_z} \cos\left(\frac{n\pi x}{L_x}\right)\cos\left(\frac{m\pi y}{L_y}\right) \\ &\quad \times \cos\left(\frac{k\pi z}{L_z}\right)\cos\left(\frac{n\pi x_s}{L_x}\right)\cos\left(\frac{m\pi y_s}{L_y}\right)\cos\left(\frac{k\pi z_s}{L_z}\right) \\ &\quad \times E_\alpha\left\{-\left[\left(\frac{n\pi}{L_x}\right)^2+\left(\frac{m\pi}{L_y}\right)^2+\left(\frac{k\pi}{L_z}\right)^2\right]K_\alpha t^\alpha\right\}, \end{aligned} \tag{16}$$

where E_α is the Mittag–Leffler function[52] with series expansion

$$E_\alpha(z) = \sum_{k=0}^{\infty} \frac{z^k}{\Gamma(\alpha k+1)}. \tag{17}$$

2.4. The ensemble-averaged MSD for fractional diffusion

The initial positions x_s, y_s, and z_s are also the stochastic variables. In the equilibrium state, the ensemble-averaged MSD should be independent on the x_s, y_s, and z_s,

$$\begin{aligned} \langle r^2(t)\rangle &= \frac{1}{L_xL_yL_z}\int_0^{L_x}\int_0^{L_y}\int_0^{L_z} \mathrm{d}x_s\mathrm{d}y_s\mathrm{d}z_s \int_0^{L_x}\int_0^{L_y}\int_0^{L_z}\mathrm{d}x\mathrm{d}y\mathrm{d}z \\ &\quad \times[(x-x_s)^2+(y-y_s)^2+(z-z_s)^2]P(\boldsymbol{r};t) \\ &= \frac{1}{6}(L_x^2+L_y^2+L_z^2) \\ &\quad -\frac{16}{\pi^4}\left\{L_x^2\sum_{k_x=0}^{\infty}\frac{1}{(2k_x+1)^4}E_\alpha\left\{-\frac{\pi^2(2k_x+1)^2}{L_x^2}K_\alpha t^\alpha\right\}\right. \\ &\quad +L_y^2\sum_{k_y=0}^{\infty}\frac{1}{(2k_y+1)^4}E_\alpha\left\{-\frac{\pi^2(2k_y+1)^2}{L_y^2}K_\alpha t^\alpha\right\} \\ &\quad \left.+L_z^2\sum_{k_z=0}^{\infty}\frac{1}{(2k_z+1)^4}E_\alpha\left\{-\frac{\pi^2(2k_z+1)^2}{L_z^2}K_\alpha t^\alpha\right\}\right\}, \end{aligned} \tag{18}$$

when t is large, the ensemble-averaged MSD reaches a constant $(L_x^2+L_y^2+L_z^2)/6$.

2.5. The exact solution of the ensemble average of time-averaged MSD

Let $P_j(x,y,z,x_s,y_s,z_s)$, which is governed by the 3D Fick's diffusion equation, Eq. (7), be the probability of a walker from x_s, y_s, z_s to x, y, z after j jump events, and $\chi_j(\Delta,t_s)$ be the probability of a walker making j jump events in the time interval Δ starting from t_s. We can then express the probability of CTRW with two independent stochastic processes, which are for the displacements and the waiting times respectively, as[41,51]

$$P(x,y,z,x_s,y_s,z_s;t_s+\Delta,t_s) = \sum_{j=0}^{\infty} P_j(x,y,z,x_s,y_s,z_s)\chi_j(\Delta,t_s). \tag{19}$$

The ensemble-averaged MSD in $[t_s,t_s+\Delta]$ can be calculated using $P(x,y,z,x_s,y_s,z_s;t_s+\Delta,t_s)$. Therefore, by using Eq. (19), one can get

$$\begin{aligned} &\langle[\boldsymbol{r}(t_s+\Delta)-\boldsymbol{r}(t_s)]^2\rangle \\ &= \int_V [\boldsymbol{r}(t_s+\Delta)-\boldsymbol{r}(t_s)]^2 P(x,y,z,x_s,y_s,z_s;t_s+\Delta,t_s)\,\mathrm{d}\boldsymbol{r} \\ &= \sum_{j=0}^{\infty}\langle r^2(j)\rangle\chi_j(\Delta,t_s). \end{aligned} \tag{20}$$

Noting that $\langle r^2(j)\rangle$ in Eq. (20) can be found by substituting $P(x,y,z,x_s,y_s,z_s;t_s+\Delta,t_s)$ with $P_j(x,y,z,x_s,y_s,z_s)$ in Eq. (10), we then find the ensemble average of time-averaged MSD for $\Delta \le T$ as

$$\langle\overline{\delta^2}(\Delta,T)\rangle = \frac{1}{T-\Delta}\sum_{j=0}^{\infty}\langle r^2(j)\rangle\int_0^{T-\Delta}\mathrm{d}t_s\chi_j(\Delta,t_s). \tag{21}$$

Let $w(t)$ be the PDF of waiting time, so in a certain time span $[t_s,t_s+\Delta]$, the probability of making j jumps is the the product of two parts, making $j-1$ jumps in a shorter time interval $[t_s,t_s+t]$ and finding a waiting time $\Delta-t$, then integrated over all possible t. Specifically, the probability of making $n \ge 2$ jumps in the time span $[t_s,t_s+\Delta]$ is

$$\chi_j(\Delta,t_s) = \int_0^{\Delta}\chi_{j-1}(t,t_s)w(\Delta-t)\,\mathrm{d}t. \tag{22}$$

Likewise, the probabilities of making one or no jump can be given respectively as

$$\chi_1(\Delta,t_s) = \int_0^{\Delta} w_1(t,t_s)w(\Delta-t)\,\mathrm{d}t, \tag{23}$$

$$\chi_0(\Delta,t_s) = 1-\int_0^{\Delta} w_1(t,t_s)\,\mathrm{d}t. \tag{24}$$

After averaging over t_s and by using the Laplace transformation $\Delta \to u$, one can get for $j \geq 1$ and $j = 0$

$$\begin{cases} \overline{\chi_j}(u) = \frac{1-w(u)}{u}[w(u)]^{j-1}\overline{w_1}(u), \\ \overline{\chi_0}(u) = [1-\overline{w_1}(u)]/u. \end{cases} \tag{25}$$

Now the ensemble average of time-averaged MSD, Eq. (21), can be expressed in the Laplace representation. Using the geometrical series, the Laplace representation of $\langle\overline{\delta^2}\rangle$ within the confined CTRW is given by

$$\langle\overline{\delta^2}(u)\rangle = \frac{\overline{w_1}(u)}{u}\frac{1-w(u)}{w(u)}\sum_{i=0}^{\infty}\frac{\gamma_i}{1-q_i w(u)}. \tag{26}$$

For a PDF of waiting time distributed like $w(t) = \alpha/(1+t)^{1+\alpha}$, its Laplace transformation is

$$w(u) \approx \alpha\, \mathrm{e}^u u^\alpha\left(\Gamma(-\alpha) + \frac{\mathrm{e}^{-u}u^{-\alpha}}{\alpha}\right) \approx 1 - \Gamma(1-\alpha)u^\alpha. \tag{27}$$

The initial waiting time distribution can be approximated as $\overline{w_1}(u) \approx (ut)^{\alpha-1}/\Gamma(1+\alpha)$, which is an approximation that is valid when $u \gg T^{-1}$. Taking into account only the terms $n = m = k = 0$, one can get

$$\begin{aligned}\langle r^2(t)\rangle \;=\; & \frac{L_x^2+L_y^2+L_z^2}{6} + \frac{16L_x^2}{\pi^4}\exp\left[-\frac{\pi^2 Dt}{L_x^2}\right] \\ & + \frac{16L_y^2}{\pi^4}\exp\left[-\frac{\pi^2 Dt}{L_y^2}\right] + \frac{16L_z^2}{\pi^4}\exp\left[-\frac{\pi^2 Dt}{L_z^2}\right],\end{aligned} \tag{28}$$

and compare it with

$$\langle r^2(j)\rangle \approx \gamma_0 q_0^j + \gamma_1 q_1^j + \gamma_2 q_2^j + \gamma_3 q_3^j, \tag{29}$$

one can get

$$\begin{cases} \gamma_0 = (L_x^2+L_y^2+L_z^2)/6, \quad q_0 = 1, \\ \gamma_1 = -L_x^2/6, \quad q_1 = \exp\left(-\frac{\pi^2\langle\delta r^2\rangle}{2L_x^2}\right), \\ \gamma_2 = -L_y^2/6, \quad q_2 = \exp\left(-\frac{\pi^2\langle\delta r^2\rangle}{2L_y^2}\right), \\ \gamma_3 = -L_z^2/6, \quad q_3 = \exp\left(-\frac{\pi^2\langle\delta r^2\rangle}{2L_z^2}\right). \end{cases} \tag{30}$$

So we have

$$\begin{aligned}\langle\overline{\delta^2}(u)\rangle \;=\; & \frac{u^{\alpha-2}}{6\Gamma(1+\alpha)T^{1-\alpha}}\left[L_x^2\frac{1-q_1}{1-q_1+q_1\Gamma(1-\alpha)u^\alpha}\right. \\ & + L_y^2\frac{1-q_2}{1-q_2+q_2\Gamma(1-\alpha)u^\alpha} \\ & \left. + L_z^2\frac{1-q_3}{1-q_3+q_3\Gamma(1-\alpha)u^\alpha}\right].\end{aligned} \tag{31}$$

By the reason $\langle\delta r^2\rangle \ll L_x^2$ (L_y^2, L_z^2), we have $q_1 \approx 1 - \pi^2\langle\delta r^2\rangle/(2L_x^2)$, $q_2 \approx 1 - \pi^2\langle\delta r^2\rangle/(2L_y^2)$, and $q_3 \approx 1 - \pi^2\langle\delta r^2\rangle/(2L_z^2)$. In Eq. (31), we ignore more high-order terms than u^α after the reduction of fractions to a common denominator, then obtain

$$\langle\overline{\delta^2}(u)\rangle = \frac{L_x^2+L_y^2+L_z^2}{6}\frac{u^{\alpha-2}}{\Gamma(1+\alpha)T^{1-\alpha}}\frac{1}{1+(\tau_c u)^\alpha}, \tag{32}$$

in which

$$\tau_c = \left(\frac{L_x^2+L_y^2+L_z^2}{\pi^2 K_\alpha}\right)^{1/\alpha}, \quad K_\alpha = \frac{\langle\delta r^2\rangle}{2\Gamma(1-\alpha)}.$$

Taking the inverse Laplace transformation for Eq. (32) and integration with the use of $\int_0^z E_{\alpha,\beta}(\lambda t^\alpha)t^{\beta-1}\mathrm{d}t = z^\beta E_{\alpha,\beta+1}(\lambda z^\alpha)$, $\beta > 0$,[52] we obtain the ensemble average of time-averaged MSD as

$$\langle\overline{\delta^2}(\Delta)\rangle = \frac{L_x^2+L_y^2+L_z^2}{6}\frac{\Delta}{\Gamma(1+\alpha)\tau_c^\alpha T^{1-\alpha}}E_{\alpha,2}[-(\Delta/\tau_c)^\alpha], \tag{33}$$

here the two-parameter function of the Mittag–Leffler type is defined by the series expansion[52]

$$E_{\alpha,\beta}(z) = \sum_{k=0}^{\infty}\frac{z^k}{\Gamma(\alpha k+\beta)}, \quad (\alpha > 0,\ \beta > 0). \tag{34}$$

From Eq. (33), we can evaluate in two limiting cases, corresponding to $\Delta \gg \tau_c$, the long Δ behavior, and $\Delta \ll \tau_c$, the short Δ behavior.[41,47,53] First, we start with the case $\Delta \gg \tau_c$. By utilizing the asymptotic behaviour of the Mittag–Leffler function: $E_{\alpha,2}[-(\Delta/\tau_c)^\alpha] \sim 1/[\Gamma(1-\alpha)(\Delta/\tau_c)^\alpha]$, when $\Delta \gg \tau_c$ and $0 < \alpha < 1$,[54] we conclude that

$$\langle\overline{\delta^2}(\Delta)\rangle \approx \frac{(L_x^2+L_y^2+L_z^2)}{6\Gamma(1+\alpha)\Gamma(2-\alpha)T^{1-\alpha}}\Delta^{1-\alpha}. \tag{35}$$

Noting that equation (35) is valid on the condition $\Delta \gg \tau_c$. In the derivation of Eq. (35), we use the notion $\overline{w_1}(u)$ which is derived from the initial waiting time probability density $w_1(t,t_s)$ averaged over t_s in the time interval $[0, T-\Delta]$[41] and then the Laplace Transformation, $\Delta \to u$. Here t_s is the aging time. The aging effect is an observed fact in experiments[56–58] and not a fantasy of theory.

For the case $\Delta \ll \tau_c$, we can put the series expansion of the Mittag–Leffler function $E_{\alpha,\beta}[-(m/\tau_c)^\alpha] = \sum_{n=0}^{\infty}[-(m/\tau_c)^\alpha]^n/(\Gamma(\beta+n\alpha))$ into use. Removing the high-order items, which can be neglected when $\Delta \ll \tau_c$, and keep $n = 0$ item, we obtain

$$\langle\overline{\delta^2}(\Delta)\rangle \approx \frac{(L_x^2+L_y^2+L_z^2)}{6\Gamma(1+\alpha)\tau_c{}^a T^{1-\alpha}}\Delta. \tag{36}$$

Taking $\tau_c = [(L_x^2+L_y^2+L_z^2)/(\pi^2 K_\alpha)]^{1/\alpha}$ into consideration, we find that

$$\langle\overline{\delta^2}(\Delta)\rangle \approx \frac{\pi^2 K_\alpha}{6\Gamma(1+\alpha)T^{1-\alpha}}\Delta. \tag{37}$$

Equation (37) is valid for $\Delta \ll \tau_c$.

3. Numerical simulation

3.1. CTRW simulations

We simulate CTRW trajectories of unbiased random walks in three dimensions with the reflecting boundaries $1 \le x \le 31$, $1 \le y \le 21$, and $1 \le z \le 11$. The subdiffusion exponent is $\alpha = 0.75$. The total measurement time is $T = 10^8$. The lag time is $\Delta = 100$. The PDFs of waiting time and displacement are defined as $w(t) = \alpha/(1+t)^{1+\alpha}$ and $f(x,y,z) = [\delta(x-1)+\delta(x+1)+\delta(y-1)+\delta(y+1)+\delta(z-1)+\delta(z+1)]/6$, respectively. In Fig. 1, the time-averaged MSD $\overline{\delta^2}$ of 20 individual trajectories are denoted by thin dotted lines, which show individual time-averaged MSD remains an independent random variable. The ensemble average of time-averaged MSD is represented by a thick green dotted line, which has a distinct crossover at τ_c from $\langle\overline{\delta^2}\rangle \sim \Delta$ in a short lag time to $\langle\overline{\delta^2}\rangle \sim \Delta^{1-\alpha}$ in a long lag time, where $\tau_c = [(L_x^2+L_y^2+L_z^2)/(\pi^2 K_\alpha)]^{1/\alpha} = 10383$, and $K_\alpha = \langle\delta r^2\rangle/(2\Gamma(1-\alpha))$. The same behaviour was also obtained in previous one-dimensional simulations.[41,47,53–55]

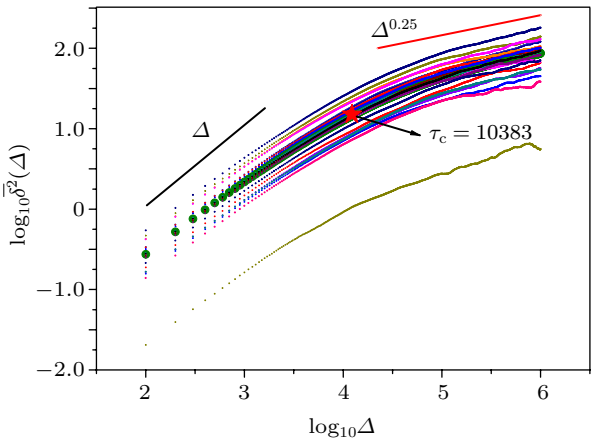


Fig. 1. (color online) CTRW simulation of time-averaged MSD as a function of Δ within 3D confined space. The walkers are entrapped in the space $1 \le x \le 31$, $1 \le y \le 21$, and $1 \le z \le 11$, with the PDF of waiting time $w(t) = \alpha/(1+t)^{1+\alpha}$ and an unbiased PFD of displacement $f(x,y,z) = [\delta(x-1)+\delta(x+1)+\delta(y-1)+\delta(y+1)+\delta(z-1)+\delta(z+1)]/6$. Here $\Delta = 100$, $\alpha = 0.75$, and the total measurement time $T = 10^8$. All simulations start at $x = 1, y = 1, z = 1$. A random waiting time t with the PDF $w(t) = \alpha/(1+t)^{1+\alpha}$ can be generated from $t = r^{-1/\alpha} - 1$, where r is a uniformly distributed random number within (0, 1). Ensemble averages of time-averaged MSD are taken from 20 trajectories (the thick green dotted line).

We then compare the CTRW simulation with the theoretical prediction given by Eq. (33). The parameters are the same as Fig. 1. As shown in Fig. 2, the simulated ensemble average of time-averaged MSD $\langle\overline{\delta^2}\rangle$ (green dots), is identical with the theory (blue dots), given by function (33). The previous works dominantly discuss the asymptotic behaviours as $T \gg \Delta \gg \tau_c$ and $\Delta \ll \tau_c$,[41,47] which well agree with our theoretical results in short Δ (from Eq. (37)) and long Δ (from Eq. (35)).

In contrast, we also compared the behaviors of the ensemble average of time-averaged MSD $\langle\overline{\delta^2}(\Delta)\rangle$ for three-dimensional diffusion, with $\langle\overline{\delta^2}_x(\Delta)\rangle$, $\langle\overline{\delta^2}_y(\Delta)\rangle$, and $\langle\overline{\delta^2}_z(\Delta)\rangle$ for only one direction diffusion of x, y, and z. In Fig. 3, the parameters are also the same as Fig. 1. However, note that the crossover points τ_c are different for every direction, because there are different boundaries in x, y, and z directions.

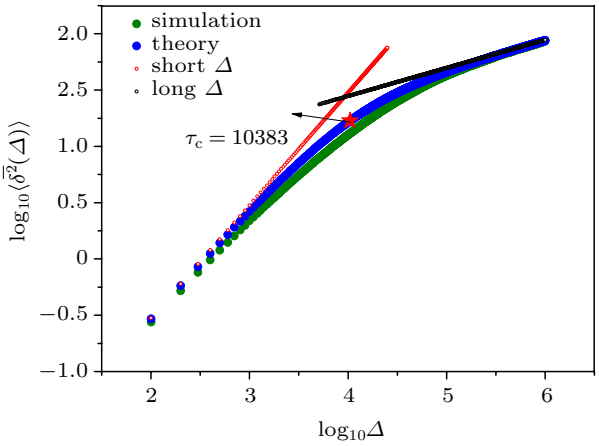


Fig. 2. (color online) Comparing CTRW simulation results with the theoretical formula of ensemble average of time-averaged MSD $\langle\overline{\delta^2}\rangle$. With $\alpha = 0.75$, $\Delta = 100$, reflecting boundaries $1 \le x \le 31$, $1 \le y \le 21$, and $1 \le z \le 11$ and the total measurement time is $T = 10^8$. The green dotted line represents the simulation, and the blue one is the theoretical result which obtains from Eq. (33) using the same parameters with numerical simulation. The red line and gray line are the theoretical results in short Δ (from Eq. (37)) and long Δ (from Eq. (35)).

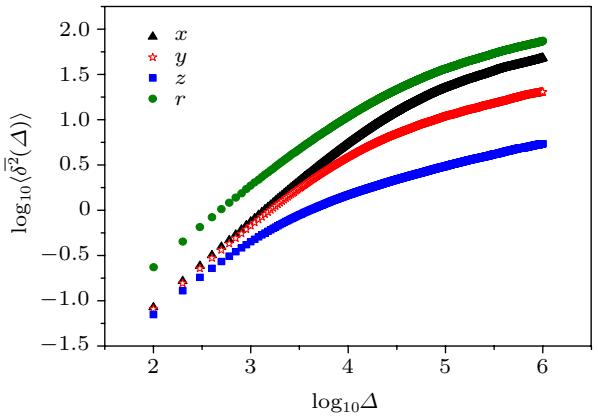


Fig. 3. (color online) Effect of boundaries on ensemble average of time-averaged MSD in three different directions. Here, the total measure time $T = 10^8$, $\alpha = 0.75$, $\Delta = 100$, and reflecting boundaries $1 \le x \le 31$, $1 \le y \le 21$, and $1 \le z \le 11$.

3.2. Comparison with experiments

In order to put our theoretical considerations to test, the results are presented to compare with the experiment in Fig. 4. The details of the experiment are reported in Ref. [39]. We treat the cellular inner membrane as reflecting boundaries in our simulation. The boundaries $1 \le x \le 31$, $1 \le y \le 11$, and $1 \le z \le 11$ indicate the relationship that x is almost three times larger than y and z, also y roughly equals z, which is observed by the experiment (Fig. 1(b) in Ref. [39]). Other parameters are as $T = 10^7$, $\alpha = 0.7$, and $\Delta = 2500$. Our results, shown in Fig. 4, are obtained by extracting x and y in the three dimensions simulation of the experiment. The simulated results are very similar to the experiment results.

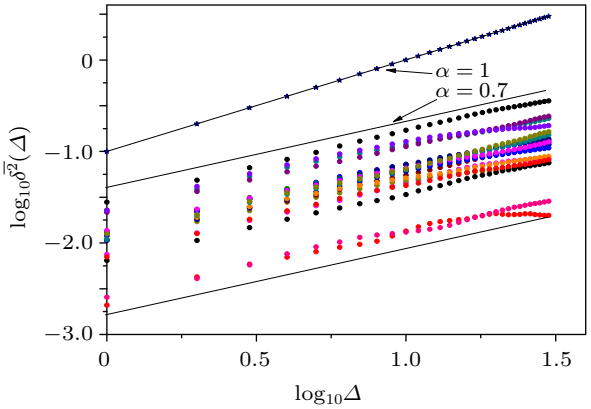


Fig. 4. (color online) Time-averaged MSD $\overline{\delta^2}$ as a function of Δ. Here the total measure time $T = 10^7$, $\alpha = 0.7$, $\Delta = 2500$, and reflecting boundaries $1 \le x \le 31$, $1 \le y \le 21$, and $1 \le z \le 11$. Our 3D simulated results are in agreement with experimental data of Fig. 2(a) in Ref. [39].

As an additional way to characterize subdiffusion and testify the CTRW, we use the data of $x(t)$ trajectories extracted from a simulation of a single particle trajectory in three dimensions to measure the power spectrum,[59] with the total measure time $T = 10^7$, also $\alpha = 0.7$, $\Delta = 2500$ and reflecting boundaries $1 \le x \le 31$, $1 \le y \le 11$, and $1 \le z \le 11$. The power spectrum of a particle is $P(f) = \left|X^2(f)\right|$, which should obey $P(f) \sim f^{-(1+\alpha)}$ when $X(f)$ is the Fourier Transform of particle position $x(t)$. In the same way, we also can calculate the power spectrum for the position $y(t)$ or $z(t)$. The simulation results from CTRW highly agree with experimental data,[39] as shown in Fig. 5.

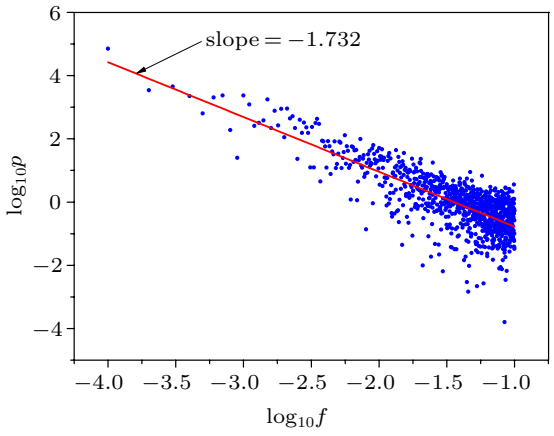


Fig. 5. (color online) Power spectrum of a single particle position $x(t)$ (blue dots). Using the Welch method gives the results of fitting slope about equal to -1.732. The total measure time is $T = 10^7$, also $\alpha = 0.7$, $\Delta = 2500$, and reflecting boundaries $1 \le x \le 31$, $1 \le y \le 11$, and $1 \le z \le 11$. Our simulated power spectrum is consistent with experiment measurement (Fig. 2(b) in Ref. [39]).

4. Conclusion

We investigate the time-averaged mean square displacement (MSD) of a 3D single particle trajectory using the continuous time random walk model (CTRW). Theoretical analysis and numerical simulation show that the CTRW model is suitable for describing the subdiffusion of mRNA in live E. coli under the confined and crowded environment. Theoretical expression of ensemble average of the time-averaged MSD is in agreement with simulated results. The simulated results are also well consistent with experimental data. The 3D trajectory and analysis can help to determine more exactly the microscopic mechanism of real single biomolecule diffusion in living cells.

References

[1] Dupont A, Gorelashvili M, Schüller V, Wehnekamp F, Arcizet D, Katayama Y, Lamb D C and Heinrich D 2013 *New J. Phys.* **15** 075008
[2] Juette M F, Rivera-Molina F E, Toomre D K and Bewersdorf J 2013 *Appl. Phys. Lett.* **102** 173702
[3] Liu S L, Li J C, Zhang Z L, Wang Z G, Tian Z Q, Wang G P and Pang D W 2013 *Scientfic Reports* **3** 2462
[4] Dupont A and Lamb D C 2011 *Nanoscale* **3** 4532
[5] Ruthardt N, Lamb D C and Bräuchle C 2011 *Mol. Ther.* **19** 1199
[6] Thompsona M A, Casolarib J M, Badieirostamia M, Brownb P O and Moernera W E 2010 *Proc. Natl. Acad. Sci.* **107** 17864
[7] Wang X L, Zhang X H, Wei K J, Sun B and Li M 2007 *Acta Phys. Sin.* **57** 3905 (in Chinese)
[8] Wells N P, Lessard G A, Goodwin P M, Phipps M E, Cutler P J, Lidke D S, Wilson B S and Werner J H 2010 *Nano Lett.* **10** 4732
[9] Sun Y, McKenna J D, Murray J M, Ostap E M and Goldman Y E 2010 *Nano Lett.* **10** 4732
[10] Bräuchle C, Lamb D C and Michaelis J 2010 *Single Particle Tracking and Single Molecule Energy Transfer* (Weinheim: Wiley-VCH)
[11] Phillips R, Kondev J and Theriot J 2009 *Physical Biology of the Cell* (Garland Science, Taylor and Francis Group LLC)
[12] Höfling F and Franosch T 2013 *Rep. Prog. Phys.* **76** 046602
[13] Sokolov I M 2012 *Soft Matter* **8** 9043
[14] Barkai E, Garini Y and Metzler R 2012 *Phys. Today* **65** 29
[15] Burov S, Jeon J, Metzler R and Barkai E 2011 *Phys. Chem. Chem. Phys.* **13** 1800
[16] Hellmann M, Klafter J, Heermann D W and Weiss M 2011 *J. Phys.: Condens. Matter* **23** 234113
[17] Mandelbrot B B and Ness J W V 1968 *SIAM Rev.* **10** 422
[18] Kou S C and Xie X S 2004 *Phys. Rev. Lett.* **93** 180603
[19] Goychuk I 2007 *Phys. Rev. E* **76** 040102
[20] Goychuk I 2009 *Phys. Rev. E* **80** 046125
[21] Langevin P 1908 *C. R. Hebd. Seances. Acad. Sci.* **146** 530
[22] Yang H J, Zhuo Y Z and Wu X Z 1994 *Acta Phys. Sin.* **3** 539 (in Chinese)
[23] Jeon J H and Metzler R 2010 *Phys. Rev. E* **81** 021103
[24] Min W, Luo G, Cherayil B J, Kou S C and Xie X S 2005 *Phys. Rev. Lett.* **94** 198302
[25] Montroll E W and Weiss G H 1965 *J. Math. Phys.* **6** 167
[26] Metzler R and Klafter J 2000 *Phys. Rep.* **339** 1
[27] Bouchaud J P and Georges A 1990 *Phys. Rep.* **195** 127
[28] Klafter J and Sokolov I M 2011 *First Step in Random Walks* (Oxford: Oxford University Press)
[29] Lin F and Bao J D 2011 *Chin. Phys. B* **20** 040502
[30] Liu J and Bao J D 2013 *Chin. Phys. Lett.* **30** 020202
[31] Lorentz H A 1905 *Arch. Neerl. Sci. Exact Natur.* **10** 336
[32] Havlin S and Ben-Avraham D 1987 *Adv. Phys.* **36** 695
[33] Saxton M J 1994 *Biophys. J.* **66** 394
[34] Franosch T, Höfling F, Bauer T and Frey E 2010 *Chem. Phys.* **375** 540
[35] Regner B M, Bučinić D, Domnisoru C, Bartol T M, Hetzer M W, Tartakovsky D M and Sejnowski T J 2013 *Biophys. J.* **104** 1652
[36] Elcock A H 2010 *Curr. Opin. Struct. Biol.* **20** 196
[37] He Y, Burov S, Metzler R and Barkai E 2008 *Phys. Rev. Lett.* **101** 058101
[38] Metziler R, Tejedor V, Jeon J H, He Y, Deng W H, Burov S and Barkai E 2009 *Acta Phys. Polon. B* **40** 1315
[39] Golding I and Cox E C 2006 *Phys. Rev. Lett.* **96** 098102
[40] Sokolov I M 2008 *Physics* **1** 8
[41] Neusius T, Sokolov I M and Smith J C 2009 *Phys. Rev. E* **80** 011109
[42] Jeon J H and Metzler R 2012 *Phys. Rev. E* **85** 021147
[43] Froemberg D and Barkai E 2013 *Phys. Rev. E* **87** 030104

[44] Burov S, Metzler R and Barkai 2010 *Proc. Natl. Acad. Sci.* **107** 13228
[45] Jeon J H, Tejedor V, Burov S, Barkai E, Christine S U, Kirstine B S, Lene O and Metzler R 2011 *Phys. Rev. Lett.* **106** 048103
[46] Schulz J H P, Barkai E and Metzler R 2013 *Phys. Rev. Lett.* **110** 020602
[47] Miyaguchi T and Akimoto T 2013 *Phys. Rev. E* **87** 032130
[48] Chang F X, Chen J and Huang W 2004 *Acta Phys. Sin.* **54** 1113 (in Chinese)
[49] Oldham K B and Spanier J 1974 *The Fractional Calculus* (New York: Academic Press)
[50] Metzler R and Klafter J 2000 *Physica A* **278** 107
[51] Sokolov I M, Blumen A and Klafter J 2001 *Europhys. Lett.* **175** 56
[52] Podlubny I 1999 *Fractional Differential Equation* (California: Academic Press)
[53] Jeon J H, Tejedor V and Burov S 2011 *Phys. Rev. Lett.* **106** 048103
[54] Haubold H J, Mathai A M and Saxena R K 2011 *J. Appl. Math.* **2011** 51
[55] Burov S, Jeon J H, Metzler R and Barkai E 2011 *Phys. Chem. Chem. Phys.* **13** 1800
[56] Weigela A V, Tamkunb M M and Krapfa D 2013 *Proc. Natl. Acad. Sci.* **110** E4591
[57] Burova S, Ali Tabeia S M, Huynhb T, Murrellc M P, Philipsond L H, Ricea S A, Gardela M L, Scherera N F and Dinnera A R 2013 *Proc. Natl. Acad. Sci.* **110** 19689
[58] Ali Tabeia S M, Burova S, Kima H Y, Kuznetsovd A, Huynha T, Jurellerc J, Philipsond L H, Dinnera A R and Scherera N F 2013 *Proc. Natl. Acad. Sci.* **110** 4911
[59] Mantegna R N, Stanley H E and Ebrary 2000 *An Introduction to Econophysics Correlations and Complexity in Finance* (Cambridge: Cambridge University Press)